ACS APPLIED MATERIALS & INTERFACES

LETTER

www.acsami.org

Superhydrophobic Functionalized Graphene Aerogels

Yirong Lin,[*,†,‡] Gregory J. Ehlert,[‡] Colton Bukowsky,[§] and Henry A. Sodano[†,‡]

[†]Department of Materials Science and Engineering, University of Florida, PO Box 116400, Gainesville, Florida 32611-6400, United States

[‡]Department of Mechanical and Aerospace Engineering, University of Florida, P.O. Box 116250, Gainesville, Florida 32611-6250, United States

[§]School for Engineering of Matter, Transport and Energy, Arizona State University, P.O. Box 876106, Tempe, Arizona 85287-6106, United States

ABSTRACT: Carbon-based nanomaterials such as carbon nanotubes and graphene are excellent candidates for superhydrophobic surfaces because of their intrinsically high surface area and nonpolar carbon structure. This paper demonstrates that graphene aerogels with a silane surface modification can provide superhydrophobicity. Graphene aerogels of various concentrations were synthesized and the receding contact angle of a water droplet was measured. It is shown that graphene aerogels are hydrophobic and become superhydrophobic following the application of a fluorinated surfactant. The aerogels produced for this experiment outperform previous carbon nanomaterials in creating superhydrophobic surfaces and offer a more scalable synthetic procedure for production.

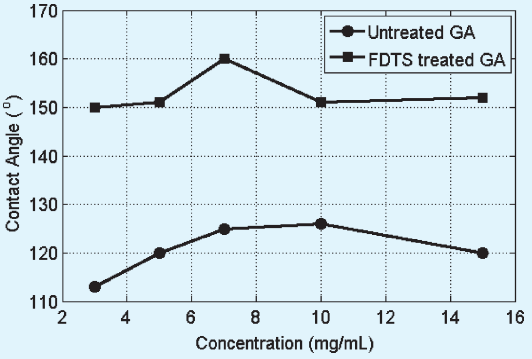

KEYWORDS: graphene, aerogel, hydrophobic, graphene oxide, superhydrophobic, macropore

Artificial hydrophobic surfaces that mimic those of natural materials, such as the lotus leaf, are extremely difficult to wet and have drawn extensive interest for self-cleaning surfaces, reduced oxidation, and improved efficiency of marine vessels.[1−5] In the case of the lotus leaf, the hydrophobicity can be attributed to both the microscale morphology of the surface roughness and a coating of nonpolar, epicuticular wax.[2,3] Likewise, synthetically prepared hydrophobic surfaces can be enhanced through increased surface roughness or chemical processes that lower the surface energy.[2]

Extensive research has been performed to mimic the natural design of these surfaces by utilizing high surface roughness micro/nanostructures along with a low surface energy coating.[6] Several methods to artificially create a high surface roughness have been reported, including solidification of alkylketene dimer wax with a fractal surface,[7] lithographic techniques for fabricating patterned nanostructures on silicon wafers[8] and the templated growth of vertically aligned carbon nanofibers[9] or polycarbonate nanopillars.[10] Other nanowire synthesis methods such as electrohydrodynamic,[11] electrospinning,[12] sol−gel processes,[13,14] and hydrothermal growth[15] are also widely used to enhance surface roughness by growing materials at the nanoscale. The hydrophobicity of high surface roughness materials can be further enhanced with the addition of a low surface energy coating.[6] To date, numerous coatings have been utilized to fabricate the superhydrophobic films, with the most widely used materials including self-assembled monolayer of alkanethiols,[16] organosilanes,[17,18] fatty acids[19] and poly(tetrafluoroethylene) (PTFE).[20] Of the materials developed for superhydrophobic structures, carbon-based nanomaterials such as carbon nanofibers (CNF),[9] carbon nanotubes (CNT),[3,21] and graphene[20] have received extensive attention because of their high surface roughness and low density. Graphene is an ideal two-dimensional material with higher specific surface area than CNFs or CNTs, which is suitable for the formation of microscale surface roughness for a hydrophobic surface.

Graphene has been developed to create hydrophobic surfaces; however most techniques simply employ graphene as a thin nonpolar surface layer rather than taking advantage of the opportunities for high surface roughness. Shin et al.[22] prepared graphene sheets on a flat substrate through epitaxial growth on SiC and showed that the water contact angle could be increased from 69° on bare SiC to 92° on graphene. Wang et al.[23] chemically reduced aqueous solutions of GO with hydrazine and observed that the contact angle of the graphene thin film reached 127°, compared to 98° for crystalline graphite. Rafiee et al.[20] produced surface-functionalized graphene with sonication in water or acetone to form superhydrophilic or superhydrophobic surfaces on various substrates. It was shown that the water contact angle of graphene isolated in acetone and then deposited on gold, highly ordered pyrolytic graphite (HOPG) and aluminum substrates could reach 160, 150, and 140° respectively.

Aerogels have high porosity, large surface area, and extremely low bulk density, which makes them a promising candidate for superhydrophobic surfaces in many new applications.[24] Research related to hydrophobic aerogels has been mainly focused on silica

Received: April 29, 2011
Accepted: June 29, 2011
Published: June 29, 2011

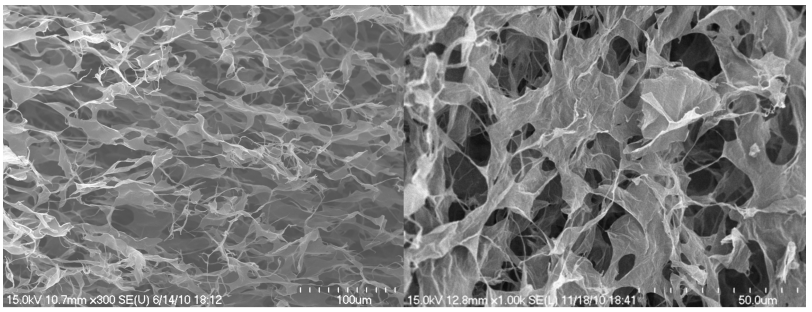

(a) (b)

Figure 1. Scanning electron microscope images of graphene aerogel from solution of 7 mg/mL: (a) without surface treatment (b) with modification of FDTS.

aerogels, which are generally fabricated through a supercritical drying process and have contact angles ranging from 100 to 150°.[24−27] Although superhydrophobicity could be achieved, the complex and time-consuming fabrication process offers opportunities for new materials to alleviate some of these difficulties. Recently, graphene aerogels have been developed to enhance the electrical conductivity for high-surface-area graphene-based electrodes for device application such as supercapacitor or lithium ion battery.[28,29] The high specific surface area and percolated network of graphene aerogels enables the material to transport and store charge with very low bulk density. Graphene aerogels are simple and inexpensive to fabricate on both laboratory and industrial scale. The production process does not require complicated procedures such as catalyst seeding or lithographic patterning of the substrate, high-temperature chemical vapor deposition or post processing to remove impurities or catalysts.[28,29]

This paper proposes a novel superhydrophobic graphene aerogel (GA) with extremely low bulk density and high water contact angle. Graphene aerogels offer lower density and simpler processing than other superhydrophobic surfaces developed using vertically aligned CNT or silica aerogels. This work demonstrates that the GA is naturally hydrophobic because of the high surface roughness; following the application of a fluorinated silane, it becomes superhydrophobic with the water contact angle reaching 160°. The superhydrophobic aerogel could be a strong candidate for self-cleaning surfaces or water repelling applications where low bulk density is important, without the complex chemical vapor deposition or supercritical drying required by alternative materials.

The graphene oxide (GO) was synthesized using the modified Hummers' method.[30,31] Aqueous dispersions of GO were prepared by stirring GO into ultrapure water (>18 MΩ cm) with concentrations ranging from 3 to 15 mg/mL followed by brief sonication (Branson 2510). The solution was then frozen using methanol and dry ice and freeze-dried to form the graphene oxide aerogel (GOA).[32] The GOA was then thermally reduced in an argon atmosphere at 1050 °C for 5 min with temperature ramp of ranging from 5 °C/min for low concentration samples to 1 °C/min for high concentration samples. Excessively high ramp rates can cause deflagration of the material. The morphology and open pore structure of the aerogel is preserved during thermal reduction; thus the surface roughness and removal of the hydroxyl, carbonyl, carboxylic acid and epoxide functional groups renders the surface hydrophobic. To further enhance the hydrophobicity of the structure, 0.2 mL of a solution prepared by dissolving 0.1 mL of 1H,1H-2H,2H perfluorodecyl-trichlorosilane (FDTS, 96%, Alfa) in 30 mL hexane (anhydrous, 99.9%, Fisher) was applied to the GA surface and allowed to dry overnight in ambient conditions. The silane treatment had the effect of lowering the surface energy of the GA to assist in creating a superhydrophobic surface.[33] Field emission scanning electron microscopy (FESEM, Hitachi-4700) was used to observe the morphology of the GA surface. Atomic force microscopy (AFM, Digital Instruments/Veeco MultiMode) was utilized in tapping mode to analyze the morphology of the individual graphene oxide sheets and ensure that single layer sheets were used. Water contact angle measurements were performed at room temperature with deionized water using a contact angle goniometer (Rame-Hart Goniometer, model 250). All X-ray photoelectron spectroscopy (XPS) experiments were performed with a pressure of less than 1.5×10^{-9} mbar with data collected on a VG ESCALAB 220i-XL and processed using CASA-XPS. All samples were excited by an Al k-α (1486 eV) monochromated X-ray source and a through-the-lens electron flood gun was used to compensate any charge losses. Each high resolution curve was first fit with a Shirley background and then decomposed into 4 Gian−Lorentzian components to fit the data. The instrumentation was calibrated for peak width on a sample of commercially available highly oriented pyrolytic graphite (NT-MDT, Zelenograd, Moscow, Russia), which resulted in a peak width of 0.6 eV.

The surface morphology of two typical GA and FDTS surface modified GAs are shown in Figure 1. The pore size of the thermally reduced GA is approximately 10−50 μm while that of the FDTS treated GA is around 5−30 μm, as estimated from the images shown in Figure 1. Note that both samples shown in Figure 1 contained the same initial solution concentration of 7 mg/mL. The pore size reduction after FDTS treatment is the result of the surface tension of the FDTS/hexane solution as it is evaporated from the aerogel surface. A typical AFM topographical scan and height profile of the GO prior to freeze-drying is shown in Figure 2. The thickness of the GO is measured to be ∼0.52 nm according to the cross-section view, which is characteristic of a monolayer GO sheet.[34]

A variety of techniques such as contact angle, tilt angle and multiresonance thickness shear mode sensors have been developed to characterize superhydrophobic surfaces; however droplet contact angle is the most widely used method for its simplicity and ease of testing.[6] A surface with a contact angle ranging from 0 to 90° is defined as hydrophilic, whereas a contact angle between 90 and 180° is defined as hydrophobic, with contact angles greater than 150° being defined as superhydrophobic.[35] Unfortunately, the water droplet deformation caused by gravity is not constant with volume and larger water droplets undergo

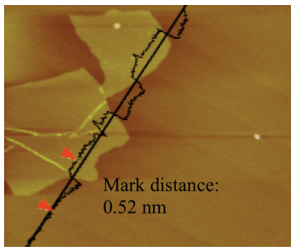

Figure 2. Atomic force microscopy image of the graphene sheets used in aerogel.

more deformation than smaller droplets, which can lead to significantly different results depending on the droplet size used.[6] This paper employs dynamic contact angle measurement by repeating the water advancing and receding as the droplet volume is increased and decreased to account for these differences. Averaged water contact angles at stable stages while receding are recorded and used to characterize the hydrophobicity of the GAs.

The hydrophobicity of a GA is believed to be a function of the dual scale roughness, the nanoscale roughness from graphene and the microscale roughness from macropores existing in the GA.[21] For most biological hydrophobic structures, such as lotus leaves, dual scale surface roughness surface have been found to be necessary to achieve superhydrophobicity.[36] This can be explained by the fact that the nanoscale roughness of (graphene) reduces the transition state energy between metastable states while microscale roughness (macropores) could result in increasing Laplace pressure.[37] Similar results have been shown in the literature to demonstrate that dual scale structures with macropore size up to hundreds of micrometers can form superhydrophobic surfaces.[38−40] Therefore, both bulk aerogel density, which controls both the surface roughness and macropore size, and modification of the surface energy have a large effect on the hydrophobicity of the sample. A typical image of a water droplet on a GA during testing is shown in Figure 3a. To vary the GA surface roughness, we tested several different density GAs with and without surface treatment and the water contact angles are shown in Figure 3b. The water contact angles of FDTS treated GAs in Figure 3b are significantly higher than those of unmodified GAs and reach values as high as 160°. The mechanism for the observed superhydrophobicity of FDTS treated GA can be explained as follows: when FDTS/hexane solution is applied onto the surface of GA, Si−Cl bonds in FDTS react with hydroxyl groups in GA to form HCl, H_2O, and Si−O bonds that graft the FDTS to the GA. The remaining C−F_2 and C−F_3 groups in FDTS then reduce the surface energy of the sample to create a superhydrophobic surface.[41] XPS analysis has been performed on both GOA and GA samples and the high resolution C1s spectrum is plotted in Figure 4. It can be seen that the GOA has significant oxidation with moieties consisting of C−O, C═O, and COOH, whereas after thermal reduction, there is a residual peak at 285.6 that, accounting for the shift in the C−C peak, can be attributed to hydroxyl and epoxide groups. The remaining hydroxyl groups act as the reaction site for grafting of the FDTS to the aerogel surface. All GAs are superhydrophobic with contact angles larger than 150° following the silane surface treatment. The water contact angle first increases then decreases with increasing aerogel density for both of the treated and untreated aerogel samples. This behavior is attributed to the

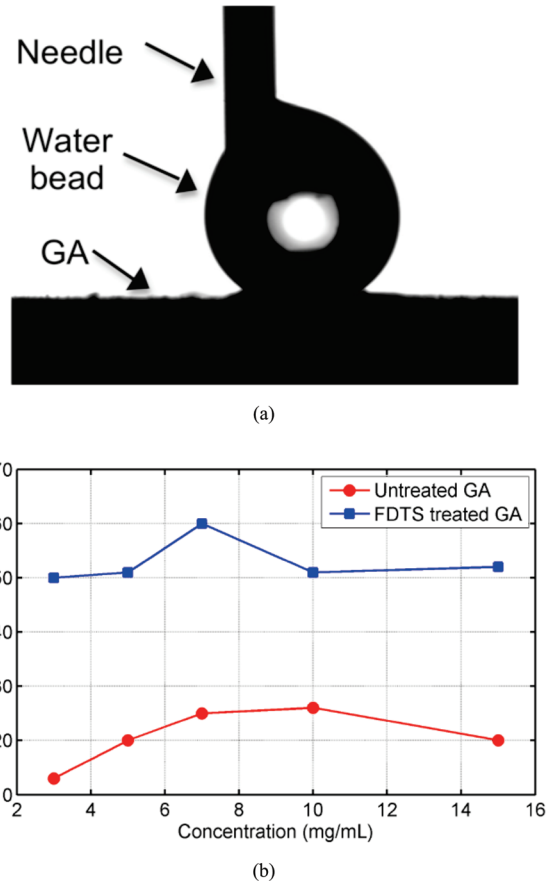

Figure 3. Water contact angle testing: (a) photograph of water contact angle of the surface of the chemically treated graphene aerogel, (b) contact angles of treat and untreated graphene aerogel surface with varies concentration.

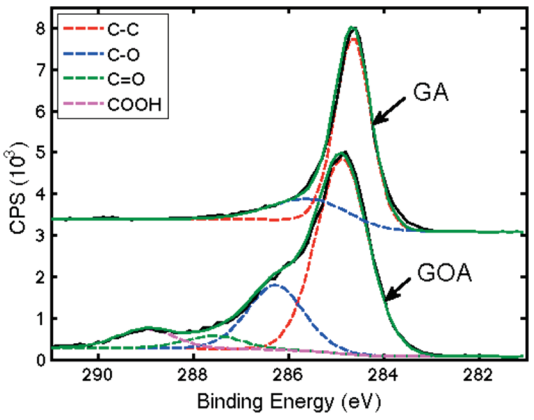

Figure 4. XPS spectra of graphene oxide aerogel and graphene aerogel.

progress of relative fraction of pores and graphene sheets. At low concentrations, the surface has a high fraction of pores compared to graphene sheets on the aerogel surface, whereas at high concentrations, the surface roughness and porosity that traps air beneath the droplet and supports it is reduced,[6] leading to an optimal density aerogel where the surface energy, porosity and surface roughness provide maximum hydrophobicity.

Li et al.[21] investigated the superhydrophobicity of a hierarchical micro/nano structure fabricated by self-assembling CNTs on polystyrene (PS) spherical colloidal crystals. It was shown that the contact angle first increased then decreased with an increasing CNT fraction. At high CNT fractions, the CNTs cover the gaps in between the spheres and thus the overall surface roughness of the entire structure decreases and less air can be trapped in the gap between PS spheres. Similarly, the GAs in this work indicate that a increasing density creates a trade-off in the overall roughness of the aerogel, which causes the maximum contact angle to occur at an intermediate graphene concentration.

In conclusion, this paper has demonstrated that graphene aerogels have the surface morphology required to create superhydrophobicity. It is shown that with the modification of a low surface energy coating on the aerogel, the water contact angle can reach as high as 160° and that any graphene aerogel with the required surface treatment can be superhydrophobic. GAs offer both production and performance advantages over other carbon or silicon-based hydrophobic surfaces; most notably the synthetic procedures to create the material are low-cost, highly scalable, and do not require supercritical drying. Following the application of a fluorinated silane agent to the surface, the hydrophobicity of graphene aerogels was comparable with all current materials utilizing carbon nanostructures such as carbon nanotubes. The superhydrophobicity of the graphene aerogel is demonstrated for the first time and the results presented here provide many opportunities for the creation for lightweight self-cleaning and anticorrosive materials.

AUTHOR INFORMATION

Corresponding Author
*E-mail: yirong.lin@ufl.edu.

ACKNOWLEDGMENT

The authors thank Chia-Jen Hsu for assistance in preparing graphene aerogel samples and Prof. Bryan Vogt for access to the contact angle goniometer.

REFERENCES

(1) Feng, L.; Li, S.; Li, Y.; Li, H.; Zhang, L.; Zhai, J.; Song, Y.; Liu, B.; Jiang, L.; Zhu, D. *Adv. Mater.* **2002**, *14*, 1857–1860.
(2) Fujishima, A.; Hashimoto, K.; Watanabe, T. *TiO2 Photocatalyst, Fundamentals and Applications*; BKC: Tokyo, 1999.
(3) Lau, K. K. S.; Bico, J.; Teo, K. B. K.; Chhowalla, M. *Nano Lett.* **2003**, *3*, 1701–1705.
(4) Erbil, H. Y.; Demirel, A. L.; Avci, Y.; Mert, O. *Science* **2003**, *299*, 1377–1380.
(5) Coulson, S. R.; Woodward, I.; Badyal, J. P. S.; Brewer, S. A.; Willis, C. *J. Phy. Chem. B* **2000**, *104*, 8836–8840.
(6) Zhang, X.; Shi, F.; Niu, J.; Jiang, Y.; Wang, Z. *J. Mater. Chem.* **2008**, *18*, 621–633.
(7) Onda, T.; Shibuichi, S.; Satoh, N.; Tsijii., K. *Langmuir* **1996**, *12*, 2125–2127.
(8) Oner, D.; McCarthy, T. J. *Langmuir* **2000**, *16*, 7777–7782.
(9) Feng, L.; Li, S.; Li, H.; Zhai, J.; Song, Y.; Jiang, L.; Zhu, D. *Angew. Chem.* **2002**, *114*, 1269–1271.
(10) Feng, L.; Song, Y.; Zhai, J.; Liu, B.; Xu, J.; Jiang, L.; Zhu, D. *Angew. Chem.* **2003**, *42*, 824–826.
(11) Feng, L.; Li, S.; Li, H.; Zhai, J.; Song, Y.; Jiang, L.; Zhu, D. *Angew. Chem.* **2002**, *41*, 4338–4341.
(12) Lim, J.; Yi, G.; Moon, J.; Heo, C.; Yang, S. *Langmuir* **2007**, *23*, 7981–7989.
(13) Tadanaga, K.; Morinaga, J.; Matsuda, A.; Minami, T. *Chem. Mater.* **2000**, *12*, 590–592.
(14) Tadana, J.; Yi, G.; Moon, J.; Heo, C.; Yang, S. *J. Am. Ceram. Soc.* **2007**, *80*, 1040–1042.
(15) Shi, F.; Chen, X.; Wang, L.; Niu, J.; Yu, J.; Wang, Z.; Zhang, X. *Chem. Mater.* **2005**, *17*, 6177–6180.
(16) Love, J. C.; Estroff, L. A.; Kriebel, L. K.; Nuzzo, R. G.; Whitesides, G. M. *Chem. Rev.* **2005**, *105*, 1103–1170.
(17) Sagiv, J. *J. Am. Chem. Soc.* **1980**, *102*, 92–98.
(18) Yang, Z.; Chiu, C.; Yang, J.; Yeh, J. *J. Micromech. Microeng.* **2009**, *19*, 085022–1−11.
(19) Hosono, E.; Fujihara, S.; Honma, I.; Zhou, H. *J. Am. Chem. Soc.* **2005**, *127*, 13458–13459.
(20) Rafiee, J.; Rafiee, M. A.; Yu, Z.; Koratkar, N. *Adv. Mater.* **2010**, *22*, 2151–2154.
(21) Li, Y.; Huang, X. J.; Heo, S. H.; Li, C. C.; Choi, Y. K.; Cai, W. P.; Cho, S. O. *Langmuir* **2007**, *23*, 2169–2174.
(22) Shin, Y. J.; Wang, Y.; Huang, H.; Kalon, G.; Wee, A.; Shen, Z.; Bhatia, C.; Yang, H. *Langmuir* **2010**, *26*, 3798–3802.
(23) Wang, S.; Zhang, Y.; Abidi, N.; Cabrales, L. *Langmuir* **2009**, *25*, 11078–11081.
(24) Lee, K; Kim, S.; Yoo, K. *J. Non-Cryst. Solids* **1995**, *196*, 18–22.
(25) Hrubesh, L. X.; Coronado, P. R.; Satcher, J. H. *J. Non-Cryst. Solids* **2001**, *285*, 328–332.
(26) Rao, A. V.; Kulkarni, M. M. *Mater. Res. Bull.* **2002**, *37*, 1667–1677.
(27) Yokogawa, H.; Yokoyama, M. *J. Non-Cryst. Solids* **1995**, *186*, 23–29.
(28) Worsley, M. A.; Pauzauskie, P. J.; Olson, T. Y.; Biener, J.; Satcher, J. H.; Baumann, T. F. *J. Am. Chem. Soc.* **2010**, *132*, 14067–14069.
(29) Worsley, M. A.; Olson, T. Y.; Lee, J. R. I.; Willey, T. M.; Nielsen, M. H.; Roberts, S. K.; Pauzauskie, P. J.; Biener, J.; Satcher, J. H.; Baumann, T. F. *J. Phy. Chem. Lett.* **2011**, *2*, 921–925.
(30) Kovtyukhova, N.; Ollivier, P. J.; Martin, B. R.; Mallouk, T. E.; Chizgik, S. A.; Buzaneva, E. V.; Gorchinskiy, A. D. *J. Chem. Mater.* **1999**, *11*, 771–778.
(31) Hummers, W.; Offeman, R. *J. Am. Chem. Soc.* **1958**, *80*, 1339.
(32) Wang, J.; Ellsworth, M. W. United States Patent US2010/0144904 A1, 2010.
(33) Li, X.; Zhang, G.; Bai, X.; Xun, X.; Wang, X.; Wang, E.; Dai, H. *Nature Nanotechnol.* **2008**, *3*, 538–542.
(34) Si, Y.; Samulshi, E. T. *Nano Lett.* **2008**, *8*, 1679–1682.
(35) Vogler, E. A. *Adv. Colloids Interfaces* **1998**, *74*, 69–117.
(36) Roach, P.; Shirtcliffe, N. J.; Newton, M. I. *Soft Matter* **2008**, *4*, 224–240.
(37) Gao, L.; McCarthy, T. J. *Langmuir* **2006**, *22*, 2966–2967.
(38) Wang, S.; Song, Y.; Jiang, L. L. *Nanotechnology* **2007**, *18*, 015103.
(39) Wagterveld, R. M.; Berendsen, C. W. J.; Bouaidat, S.; Jonsmann, J. *Langmuir* **2006**, *22*, 10904–10908.
(40) Gao, L.; McCarthy, T. J. *Langmuir* **2006**, *22*, 6234–6237.
(41) Bu, L. Y. Y.; Oei, S. P. *Appl. Surf. Sci.* **2010**, *256*, 6699–6704.